Journal of Innovative Research (JIR)

ISSN: 2837-6706 (ONLINE)

VOLUME 3 ISSUE 2 (2025)

PUBLISHED BY
E-PALLI PUBLISHERS, DELAWARE, USA

Journal of Innovative Research (JIR)

Volume 3 Issue 2, Year 2025
ISSN: 2837-6706 (Online)
DOI: https://doi.org/10.54536/jir.v3i2.4468
https://journals.e-palli.com/home/index.php/jir

First-Principles investigation of the Electronic and Optical Properties of Cs-Doped $FAPbI_3$ Halide Perovskite Solar Cell

Collins E. Ouserigha[1*], Ayibapreye K. Benjamin[2]

Article Information

Received: February 01, 2025

Accepted: March 06, 2025

Published: May 19, 2025

Keywords

Absorption, Band Gap, $FAPbI_3$, Shockley-Queisser, Tandem Solar

ABSTRACT

Despite their promising power conversion efficiency, formamidinium lead iodide ($FAPbI_3$) perovskite solar cells have phase instability and moderate efficiency. Doping with cesium (Cs) has been demonstrated to improve the stability of the photoactive α-$FAPbI_3$ phase as well as increase the efficiency. The effect of Cs doping on the electronic and optical characteristics of $FAPbI_3$ is examined in this work using first-principles density functional theory (DFT) computations. Our findings demonstrate that the addition of Cs causes minor alterations in the electronic structure, such as shifts in the bandgap and adjustments to the effective masses. In addition, we examine the optical absorption characteristics of Cs-doped $FAPbI_3$, offering information on how doping might affect device performance. Due to its 1.28 eV band gap, which is within the Shockley-Queisser limit, the 12.5% Cs-doped $FAPbI_3$ is appropriate for use in tandem solar cells. These results provide useful theoretical direction for the logical design and optimization of stable and high-performing Cs-doped $FAPbI_3$ perovskite solar cells.

INTRODUCTION

The remarkable optoelectronic characteristics of organic-inorganic halide perovskites, including their long carrier diffusion lengths, variable bandgaps, and high absorption coefficients, have made them attractive candidates for next-generation solar applications. Of them, formamidinium lead iodide ($FAPbI_3$) has attracted a lot of interest because of its excellent conversion efficiencies and perfect bandgap for solar energy conversion. The stability and performance of the device are severely limited by the black, photoactive α-$FAPbI_3$ phase (in cubic structure), which is metastable at ambient temperature and easily transforms into the non-perovskite yellow δ-phase (in hexagonal structure) (Li *et al.*, 2018; Zheng *et al.*, 2022). The narrow band gap (~1.48 eV) $FAPbI_3$ perovskite solar cells have demonstrated substantially lower efficiencies (less than 18%), despite the fact that high-efficiency solar cells with power conversion efficiency (PCE) around 25% have been created based on FA-involved mixed-cation/anion perovskites (Zhang *et al.*, 2019; Zheng *et al.*, 2022). Cation doping is one way to increase the stability of α-$FAPbI_3$. Cesium (Cs) doping has demonstrated special potential in boosting solar performance, prolonging carrier lifetimes, and stabilizing the black phase (Li *et al.*, 2018; Zheng *et al.*, 2022). Even with advancements in experimentation, a basic comprehension of the mechanisms by which Cs doping affects the electronic and optical characteristics of $FAPbI_3$ is still essential for future improvement (Duan *et al.*, 2023).

In this work, the electronic and optical characteristics of Cs-doped $FAPbI_3$ are investigated using first-principles density functional theory (DFT) computations. We methodically investigate how the addition of Cs affects the material's optical and electronic characteristics. Our findings shed important light on the bandgap shifts, effective masses, and optical absorption characteristics of the electrical structural changes brought about by Cs doping. These findings can direct future research efforts in the development of tandem cells and high-performance, stable Cs-doped $FAPbI_3$ perovskite solar cells.

LITERATURE REVIEW

Due to their remarkable optoelectronic characteristics, including its long carrier diffusion lengths, high absorption coefficients, and variable band gaps, halide perovskites have become attractive candidates for next-generation solar cells. Because of its higher power conversion efficiency than other perovskites, such as methylammonium lead iodide ($MAPbI_3$), formamidinium lead iodide ($FAPbI_3$) has demonstrated significant promise among these. Nevertheless, $FAPbI_3$'s phase instability and poor thermal stability limit its usefulness. Many studies have been conducted to solve these constraints, and cation doping—especially with caesium (Cs)—is one promising strategy. The existing knowledge of $FAPbI_3$ perovskites, their difficulties, the effect of Cs doping, and the use of first-principles calculations in this area are all examined in this overview of the literature.

Theoretically, $FAPbI_3$ has higher power conversion efficiencies than $MAPbI_3$ due to its wider bandgap and better thermal stability (Eperon *et al.*, 2014). However, at room temperature, $FAPbI_3$ exhibits a phase transition from the desirable α-phase (perovskite) to the undesirable δ-phase (non-perovskite), which significantly degrades device performance (Liang *et al.*, 2024; Zhang *et al.*, 2023). This instability is caused by the larger size of the FA cation than MA, which causes strain within the perovskite lattice. This phase instability is a major obstacle to achieving the

[1] Department of Physics, Niger Delta University, Amassoma, Nigeria
[2] Department of Electrical/Electronics, Niger Delta University, Amassoma, Nigeria
[*] Corresponding author's e-mail: ouserigha.ec@ndu.edu.ng

full potential of $FAPbI_3$-based solar cells.

Numerous approaches, such as compositional engineering, surface passivation, and interface modification, have been investigated to increase the stability of $FAPbI_3$. According to Lu *et al.*, (2020), cation doping has been shown to be an efficient technique, particularly when used with alkali metals like Cs. By modifying the perovskite lattice, Cs inclusion can reduce strain and prevent the formation of the δ-phase. It may also affect the perovskite film's shape and grain size, which could result in less hysteresis and better charge transfer (Wu *et al.*, 2018; Strathongsian *et al.*, 2024).

The impact of Cs doping on the optical, electronic, and structural characteristics of $FAPbI_3$ has been the subject of numerous investigations. According to experimental research, adding trace amounts of Cs can greatly improve the long-term performance and phase stability of $FAPbI_3$-based solar cells (Duan *et al.*, 2024). The fundamental mechanisms of this stabilization have been better understood thanks to theoretical investigations, especially those that use first-principles computations. These investigations have demonstrated the effects of Cs doping on the electronic band structure, optical absorption characteristics, and formation energy of the various phases (Taya *et al.*, 2019).

Density functional theory (DFT)-based first-principles calculations have emerged as a crucial instrument in materials research, especially in the area of perovskite solar cells. DFT makes it possible to accurately predict material features at the atomic level, such as optical characteristics, electronic structure, and structural stability (Martin, 2020). These computations can yield important insights into how strain, doping, and other variables affect perovskite material performance. In particular, DFT calculations can be used to better understand the effects of Cs incorporation on the band gap, charge carrier effective masses, and optical absorption spectra in the context of Cs-doped $FAPbI_3$. Insights into the stabilizing mechanism can also be gained by clarifying the interactions between Cs and the $FAPbI_3$ lattice.

This work aims to explore the electronic and optical characteristics of Cs-doped $FAPbI_3$ using first-principles calculations. The goal of the study is to find out how Cs doping affects the band structure, optical absorption, and other pertinent characteristics by methodically changing the Cs concentration. The findings will help us better understand how Cs improves the bandgap and performance of solar cells based on $FAPbI_3$.

MATERIALS AND METHODS

By applying the plane-wave pseudo-potential techniques within density functional theory, which are implemented in the Quantum ESPRESSO code, several properties of $FAPbI_3$ and Cs-doped $FAPbI_3$ (figure 1) were

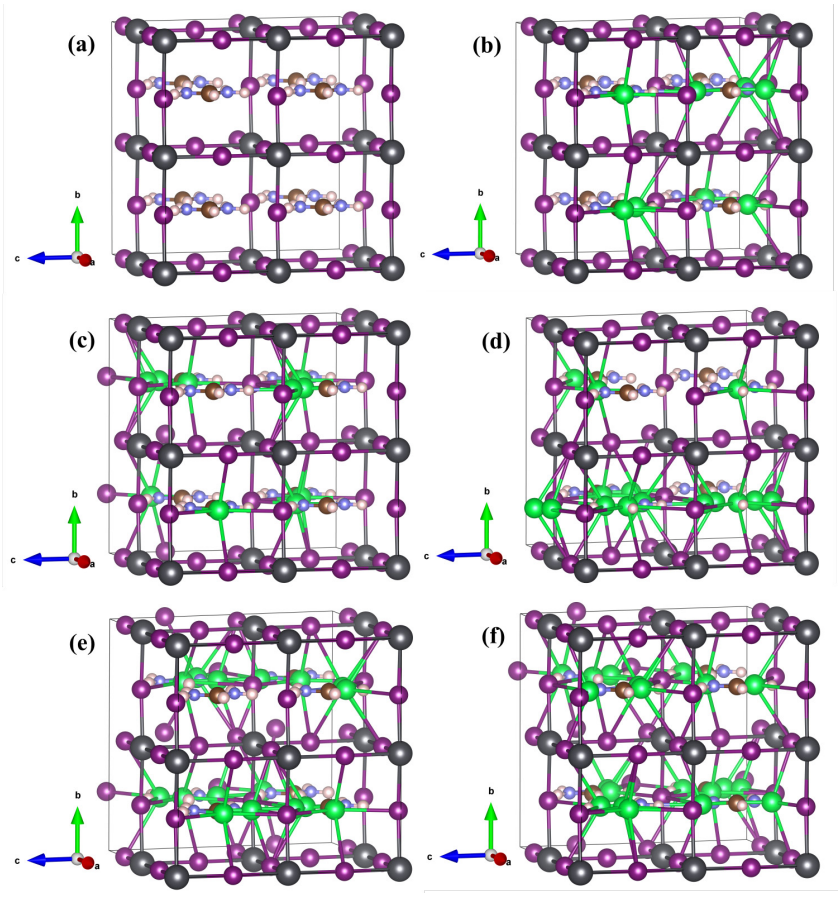

Figure 1: A 2 × 2 × 2 supercell structures of (a) $FAPbI_3$ ($CH_5N_2PbI_3$) (b) 5% Cs-doped $FAPbI_3$ (c) 12.5% Cs-doped $FAPbI_3$ (d) 15% Cs-doped $FAPbI_3$ (e) 20% Cs-doped $FAPbI_3$ (f) 25% Cs-doped $FAPbI_3$. The brown, peach, grey, black, purple and lemon coloured spheres represent Carbon, Hydrogen, Nitrogen, Lead, Iodine and Caesium atoms respectively

examined (Giannozzi *et al.*, 2020; Giannozzi *et al.*, 2017; Giannozzi *et al.*, 2009). Perdew-Burke-Ernzerhof's (PBE) generalized gradient approximation (Perdew *et al.*, 1996) was employed as the exchange correlation functional. 65.0 Ry was chosen as the kinetic-energy cutoff, and the Monkhorst-Pack (Monkhorst & Pack, 1976) k-point grid of 7 × 7 × 7 was used to sample the reciprocal space. A Gaussian smearing width of 0.002 Ry was used. For the supercell structures ($FAPbI_3$ and Cs-doped $FAPbI_3$), we geometry optimized the equilibrium structural parameters (by relaxing the lattice volume and internal ions while fixing the lattice shape) through total energy minimization with the force convergence threshold on the atoms set to 0.00038 Ry/bohr. Our first-principles calculations were performed using experimental lattice parameters (Weller, 2015) to determine the optimal local structure of $FAPbI_3$. A 2 × 2 × 2 supercell of $FAPbI_3$ was created in order to achieve Cs doping, and depending on the proportion of the composition created, Cs^+ was used to substitute some of the FA^+ ions inside the supercell (figure 1). The joint density of states (JDOS), dielectric function spectra, and absorption spectra were used to analyze the optical characteristics, while, the electronic properties were determined via density of states (DOS) and band structures. The VESTA program was used to create all of the supercell structure pictures (Momma & Izumi, 2008), and the Materials Square platform was used to perform the density functional theory (DFT) calculations (Virtual Lab., 2017).

RESULTS AND DISCUSSION

A direct bandgap at the Γ-point is visible in the band structure plot of Formamidinium Lead Triiodide ($FAPbI_3$) shown in figure 2(a), indicating that the conduction band

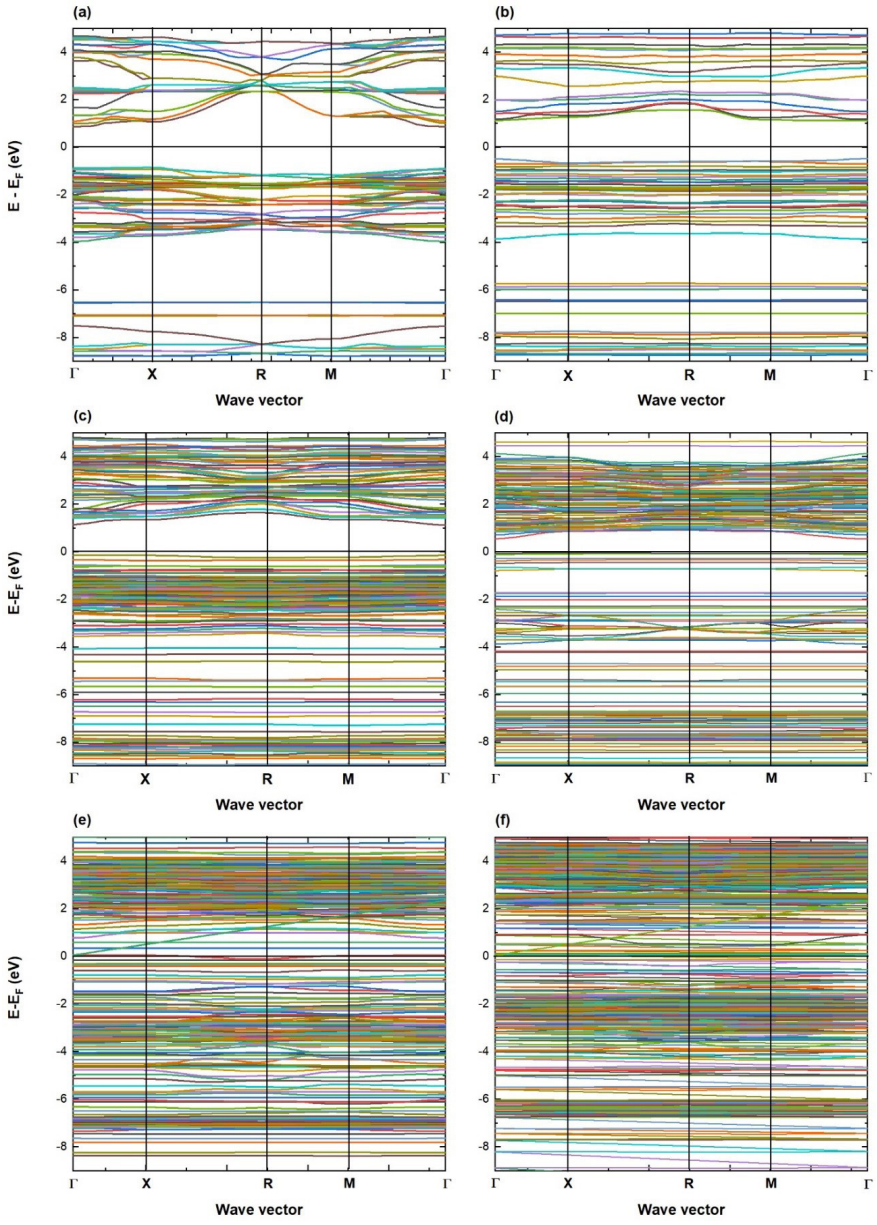

Figure 2: Band structure plots for a 2 × 2 × 2 supercell structure of: (a) $FAPbI_3$ ($CH_5N_2PbI_3$) (b) $Cs_{0.05}FA_{0.95}PbI_3$ (c) $Cs_{0.125}FA_{0.875}PbI_3$ (d) $Cs_{0.15}FA_{0.85}PbI_3$ (e) $Cs_{0.2}FA_{0.8}PbI_3$ (f) $Cs_{0.25}FA_{0.75}PbI_3$

minimum (CBM) and valence band maximum (VBM) occur at the same location in the Brillouin zone. This feature is advantageous for photovoltaic applications because it enables effective carrier generation in response to light absorption. The bandgap measured is 1.36 eV. This value aligns well with the reported bandgap of 1.45 to 1.48 eV for $FAPbI_3$ (Zheng *et al.*, 2022; Lu *et al.*, 2020). In general, we observe flat bands in the given band structures, particularly in the valence band. The valence and conduction bands are quite flat near the band edges. High carrier mobilities and enhanced photovoltaic performance are two benefits of flat bands. Furthermore, delayed carrier recombination, which can result in longer carrier lifetimes and better device performance, benefits from flat bands. The effective mass of the charge carriers (holes and electrons) is determined by the curvature of the bands close to the band edges. The flat bands imply that both electrons and holes have comparatively tiny effective masses. High solar efficiency depends on efficient carrier transport, which is made possible by a low effective mass. The influence of spin-orbit coupling is indicated by the appearance of numerous bands at the same energy level. Rashba splitting and topological effects are two intriguing phenomena that can result from this interplay.

The band structure plots for various Cesium (Cs) doping levels on the $FAPbI_3$ supercell are displayed in figures 2(b) through (f). Figure 2(b) displays 5% Cs-doped $FAPbI_3$ ($Cs_{0.05}FA_{0.95}PbI_3$). The plot's rather small bandgap of 0.98 eV raises the possibility that, in some applications, this doping level may not be enough for ideal bandgap tuning. The band structure plot for a 12.5% Cs-doping ($Cs_{0.125}FA_{0.875}PbI_3$) is displayed in Figure 2(c). The bandgap is 1.29 eV, which is marginally wider than for 5% Cs doping, suggesting that higher Cs concentration might has a beneficial impact on bandgap engineering. Given that this band gap is between 1.1 and 1.4 eV, which is the Shockley-Queisser optimum, $Cs_{0.125}FA_{0.875}PbI_3$ may have a high PCE (Lu *et al.*, 2020; Zheng *et al.*, 2022). Figures 2(d), 2(e), and 2(f) show the band structure diagrams for 15% ($Cs_{0.15}FA_{0.85}PbI_3$), 20% ($Cs_{0.20}FA_{0.80}PbI_3$), and 25% ($Cs_{0.25}FA_{0.75}PbI_3$) Cs-doping, respectively. When the doping concentration rises from 15% to 25% Cs, the band gap in these situations is zero. We restrict the Cs doping at 25% since it can cause phase segregation and degradation of the perovskite structure, even though the bandgap seems to have decreased even further.

Figures 3 (a), (b), and (c) display the density of states (DOS) plots for $FAPbI_3$, $Cs_{0.05}FA_{0.95}PbI_3$, and $Cs_{0.125}FA_{0.875}PbI_3$, respectively. The DOS clearly displays a band gap between the conduction band (CB) and the valence band (VB) in figure 3(a). According to the reported bandgap of $FAPbI_3$, the bandgap seems to be approximately 1.36 eV. Sharp peaks can be seen in the DOS, especially around the band margins. The high density of states at such energy is indicated by these peaks. There are numerous energy levels accessible for electrons and holes to inhabit when there is a large density of states. Effective charge transport may benefit from this. Van Hove singularities are a common term used to describe the strong peaks in the DOS. The curvature of the bands in the band structure is the cause of these singularities (Cao *et al.*, 2018; Regan *et al.*, 2020; Xu *et al.*, 2020). Higher density of states is a result of flatter bands. Compared to the valence band, the conduction band seems to have a higher density of states. This suggests that there are more conduction band electron energy levels available, which may result in increased carrier mobility.

The DOS curve for doping $FAPbI_3$ with 5% Cs atoms

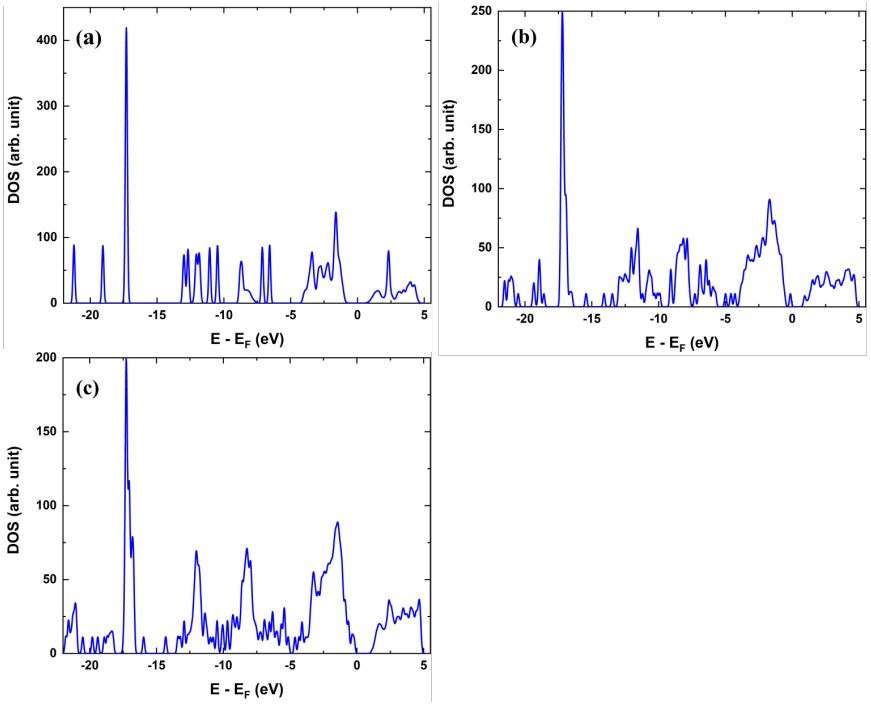

Figure 3: Density of states (DOS) plots for a 2 × 2 × 2 supercell structure of: (a) $FAPbI_3$ (CH5N2PbI3) (b) $Cs_{0.05}FA_{0.95}PbI_3$ (c) $Cs_{0.125}FA_{0.875}PbI_3$

($Cs_{0.05}FA_{0.95}PbI_3$) is displayed in Figure 3(b), and as previously mentioned, its band gap is 0.98 eV. Compared to the valence band, the conduction band appears less complex, yet it still exhibits significant structure.

Pb 6p and I 5p orbitals are most likely linked to the peaks in the conduction band. Sharp peaks in the valence and conduction bands indicate that this material's electronic states are comparatively confined. This may affect optical characteristics and carrier transport. The DOS diagram for 12.5% Cs-doped $FAPbI_3$ ($Cs_{0.125}FA_{0.875}PbI_3$) is displayed in figure 3(c). A high density of states close to the top of the valence band is indicated by the steep peak at the VB edge. Efficient conveyance of holes may be facilitated by this high density of states. A reduced density of states close to the bottom of the conduction band is suggested by the CB edge's less noticeable peak when compared to the VB edge. This might have an effect on electron transport. Within the band gap, there are a few prominent peaks. These peaks stand for confined states, which have the potential to imprison charge carriers and shorten their lifetime and mobility. Perovskite solar cells may perform worse in these mid-gap states (Elmestekawy *et al.*, 2023). The density of trap states inside the band gap can be decreased with the proper quantity of cesium inclusion. This is essential for raising the fill factor (FF) and open-circuit voltage (VOC) of perovskite solar cells. A more equal distribution of electronic states and possibly a decrease in trap states can result from cesium stabilizing the cubic crystal phase of $FAPbI_3$. According to the DOS plot, 12.5% cesium doping in $FAPbI_3$ may enhance perovskite solar cells' overall performance by: lowering the mid-gap state density, which can improve the fill factor and open-circuit voltage. stabilizing the cubic crystal phase, which may lessen trap states and result in a more even distribution of electronic states (Othman *et al.*, 2024).

As shown in figures 4(a) to (j), certain optical characteristics were computed for the supercell structures of $FAPbI_3$ and 12.5% Cs-doped $FAPbI_3$ ($Cs_{0.125}FA_{0.875}PbI_3$). The absorption spectra for $FAPbI_3$ are displayed in figure 3(a & g). In the visible spectrum, the spectra display a prominent absorption band, especially between 400 and 800 nm. Given that it shows that $FAPbI_3$ can efficiently absorb a sizable amount of the solar spectrum, this property is essential for photovoltaic applications (Imran & Khan, 2019). Around 800 nm is the absorption edge, where the absorption begins to rise sharply. This translates to a bandgap of roughly 1.55 eV (using equation (1)), which is close to the $FAPbI_3$ bandgap that has been observed. The optical characteristics of $FAPbI_3$ are anisotropic, as seen by the variations in the absorption spectra for the various polarizations (α-X, α-Y, and α-Z). The orthorhombic crystal structure of $FAPbI_3$ is most likely the cause of this anisotropy. $FAPbI_3$ is a potential material for perovskite solar cells because of its appropriate bandgap and significant absorption in the visible range. The device architecture can be optimized to enhance light absorption and charge collection by utilizing the anisotropy of the optical characteristics (Zheng *et al.*, 2022). The Urbach tail, a progressive rise in absorption beneath the bandgap, is visible in the absorption spectra. The bandgap's localized states, which can serve as recombination hubs and impair device performance, are responsible for this tail. The bandgap and absorption coefficient of $FAPbI_3$ can change with temperature, which can influence the device performance (Wright *et al.*, 2020; Elmestekawy *et al.*, 2023).

$$E(eV) = 1240/\lambda \text{ nm} \quad (1)$$

Figure 4(b & h) shows the absorption spectra for $Cs_{0.125}FA_{0.875}PbI_3$. The material's absorption edge is roughly 750 nm, corresponding to an estimated bandgap of 1.65 eV. With a peak value of approximately 0.95 million units (assuming the y-axis units are arbitrary), the absorption intensity is fairly strong. This suggests that a wide variety of visible spectrum wavelengths can be efficiently absorbed by $Cs_{0.125}FA_{0.875}PbI_3$. With Cs doping, the absorption onset moves toward shorter wavelengths, suggesting a bandgap widening. There is a small anisotropy in the absorption spectra, with the x-axis showing somewhat higher absorption than the y and z-axes. The material's crystallographic orientation or other variables may be the cause of this anisotropy. Caesium inclusion can marginally raise the bandgap of $FAPbI_3$, as was previously mentioned. A wider band gap can lessen the possibility of bandgap shrinking brought on by temperature fluctuations or halide segregation, which is advantageous for enhancing the stability of perovskite solar cells (Chen, 2022). The Urbach tail, a region of sub-bandgap absorption brought on by disorder and imperfections, can be lessened via caesium doping. This is essential for raising the fill factor (FF) and open-circuit voltage (VOC) of perovskite solar cells.

According to the absorption spectra, 12.5% Caesium doping in $FAPbI_3$ may enhance perovskite solar cells' performance in the following ways: Raising the bandgap can improve stability. lowering the Urbach tail, which may cause FF and VOC to increase (Liu *et al.*, 2022).

The absorption spectra of $Cs_{0.125}FA_{0.875}PbI_3$ are shown in Figure 4(h). Strong optical transitions at such photon energies are indicated by the plot's multiple distinct peaks in the Im ε spectrum. The bandgap of $Cs_{0.125}FA_{0.875}PbI_3$, which is located at about 1.55 eV, is the most noticeable peak. For solar cells to absorb light, this peak is essential. A noticeable increase in the Im ε at about 1.55 eV indicates the estimated bandgap of $Cs_{0.125}FA_{0.875}PbI_3$. The breadth of the peak can be used to estimate the bandgap's width. The absorption is marginally larger along the x-direction than along the y- and z-directions, indicating some anisotropy in the Im ε values. The material's crystallographic orientation or other variables may be the cause of this anisotropy. Caesium inclusion can, as previously stated, marginally expand the bandgap of $FAPbI_3$, as evidenced by a shift to higher energies in the major Im ε peak. The Urbach tail is a region of sub-bandgap absorption brought on by disorder and imperfections, and caesium doping can aid in reducing it.

As a result, the Im ε may peak more sharply and have a greater peak value.

Spectra of the dielectric function for $FAPbI_3$ are shown in Figure 4(c). $FAPbI_3$ has notable optical anisotropy, as evidenced by the dielectric function's substantial dependency on the polarization directions (x, y, and z). Given the material's orthorhombic crystal structure, this makes sense. Figure 4(i) shows the refractive index's spectra, which are related to the real part of the dielectric function (Re). Plotting indicates that photon energy and polarization direction have a considerable impact on the refractive index. The refractive index generally declines with increasing photon energy and is larger for lower photon energies (the complex index of refraction and the dielectric function). The majority of materials behave in this way. The direction of polarization also has a significant impact on the refractive index. The optical anisotropy of $FAPbI_3$ is highlighted by the varied values of n-x, n-y, and n-z at a wide range of photon energies (see figure 4(i)). The absorption coefficient and the imaginary component of the dielectric function (Im) are connected. Strong absorption peaks in specific energy ranges are visible in the plot, suggesting that $FAPbI_3$ absorbs light there. The direction of polarization also affects the locations and intensities of these absorption peaks (Radzwan *et al.*, 2019). The dielectric function's real and imaginary components reveal information about how a material reacts to electromagnetic radiation (Shen *et al.*, 2024). The refractive index is linked to the real part (ε1), whereas absorption is directly related to the imaginary part (ε2) (Radzwan *et al.*, 2019). Strong absorption that appears in the Im section of the dielectric function can be linked to the material's bandgap. It is consistent with earlier reports that the bandgap of $FAPbI_3$ is approximately 1.55 eV, as seen by the plot. Perovskite solar cells can maximize light absorption and charge collection by utilizing the optical anisotropy of $FAPbI_3$. The device performance can be improved and light absorption increased by adjusting the perovskite film's orientation or the polarization of incident light (Kaminski *et al.*, 2016).

For $Cs_{0.125}FA_{0.875}PbI_3$, the dielectric function and refractive index spectra are shown in figure 4(d) and (j), respectively. In accordance with the bandgap of $FAPbI_3$, the real part of the dielectric function (Re) exhibits a prominent positive peak at about 1.55 eV. For light trapping in solar cells, this peak denotes a high visible area refractive index, which can improve light absorption. Compared to the y and z directions, the x-direction has greater Re values, indicating some anisotropy in the optical characteristics. This anisotropy may result from the material's crystallographic orientation or from other causes. Absorption is represented by the imaginary component (Im) of the dielectric function. The bandgap absorption is represented by a strong peak that appears at about 1.55 eV. This suggests a high level of visible light absorption, which is essential for solar cells to capture light effectively. In line with the anisotropy shown in the Re values, the Im values are likewise higher for the x-direction. As previously stated, the bandgap of $FAPbI_3$ may be slightly increased by caesium inclusion, as seen by a shift in the peak locations of both Re and Im (also see the n spectra in figure 4(j)). The Urbach tail, a region of sub-bandgap absorption brought on by disorder and imperfections, can be lessened via caesium doping. This may result in a greater peak value and a sharper peak in the Im spectrum. According to the dielectric function data, 12.5% Caesium doping in $FAPbI_3$ may enhance perovskite solar cells' performance in the following ways: Because of the high refractive index, light trapping is enhanced. Stability may be improved by raising the bandgap. increasing the Re n spectrum's homogeneity, which may result in improved optical performance. lowering the Urbach tail, which may result in better open-circuit voltage (VOC) and increased light absorption (Subedi *et al.*, 2022).

Figure 4(e) displays the joint density of states (JDOS) spectrum for $FAPbI_3$. The possible electronic transitions that may contribute to optical absorption are described by the JDOS (Saleh *et al.*, 2014). Figure 4(e)'s JDOS spectrum clearly demonstrates an absorption beginning at about 1.55 eV. This is equivalent to $FAPbI_3$'s bandgap, which is an important factor for its photovoltaic uses. The JDOS spectrum shows multiple discrete absorption peaks, which are indicative of strong optical transitions at those energies. The electronic transitions between particular energy levels in the valence and conduction bands of $FAPbI_3$ are probably responsible for these peaks. Regions of high density of states, where optical transitions are more likely to occur, are shown as sharp peaks in the JDOS. The potential for excitonic effects is shown by the strong peaks in the JDOS spectrum. Bound electron-hole pairs called excitons have a big impact on a material's optical characteristics (Molas, 2023). The JDOS spectrum offers important information about $FAPbI_3$'s optical absorption characteristics, which are essential for solar cell performance. Strong absorption peaks in the visible spectrum suggest that a sizable section of the solar spectrum can be efficiently absorbed by $FAPbI_3$. In solar cells, the excitonic effects can also affect the processes of charge carrier recombination and production (Gregg, 2003). The Joint Density of States plot for $Cs_{0.125}FA_{0.875}PbI_3$ is shown in figure 4(f). Strong optical transitions at those energies are indicated by the multiple distinct peaks in the JDOS plot. The bandgap of $Cs_{0.125}FA_{0.875}PbI_3$, which is located at about 1.55 eV, is the most noticeable peak. For solar cells to absorb light, this peak is essential. At about 1.55 eV, the JDOS sharply rises, indicating the bandgap of $Cs_{0.125}FA_{0.875}PbI_3$. The breadth of the peak can be used to estimate the bandgap's width. The presence of localized states or disorder may be indicated by a slight tail that extends into the sub-bandgap region. The open-circuit voltage (VOC) and fill factor (FF) of solar cells can be impacted by the Urbach tail. Caesium doping in $FAPbI_3$ can impact its JDOS in a number of ways: As was previously indicated, the major JDOS peak may shift to higher energies as a result of a minor increase in the bandgap of $FAPbI_3$ caused by caesium inclusion. This may result in a greater peak value and a sharper peak in the JDOS.

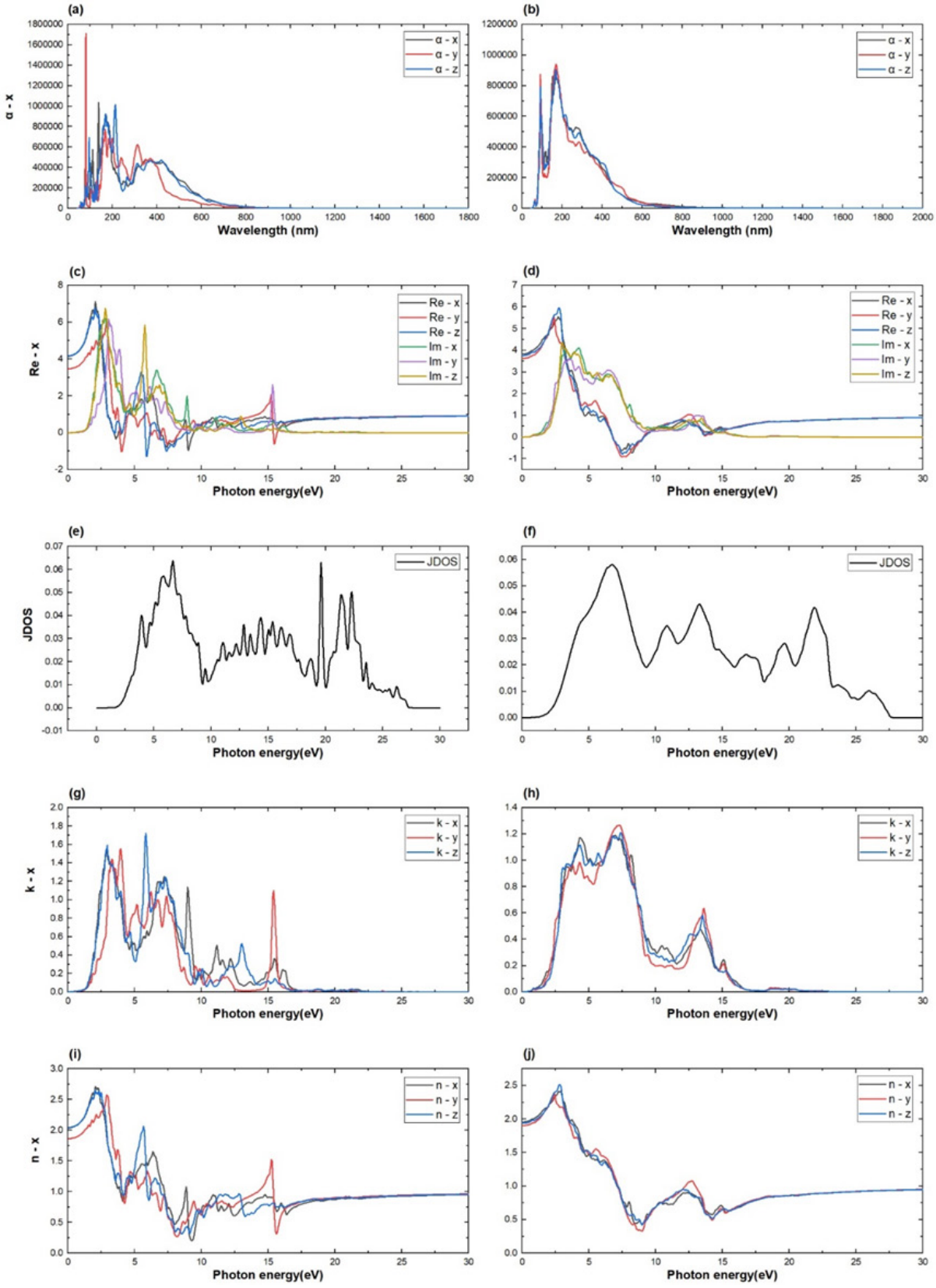

Figure 4: Optical properties plots for $FAPbI_3$ and 12.5 % Cs-doped $FAPbI_3$ (a) absorption spectra of $FAPbI_3$ (b) absorption spectra of $Cs_{0.125}FA_{0.875}PbI_3$ (c) dielectric function spectra of $FAPbI_3$ (d) dielectric function spectra of $Cs_{0.125}FA_{0.875}PbI_3$(e) joint density of states (JDOS) spectrum of $FAPbI_3$ (f) joint density of states (JDOS) spectrum of $Cs_{0.125}FA_{0.875}PbI_3$ (g) absorption spectra of $FAPbI_3$ (h) absorption spectra of $Cs_{0.125}FA_{0.875}PbI_3$ (i) refractive index spectra of $FAPbI_3$ (j) refractive index spectra of $Cs_{0.125}FA_{0.875}PbI_3$

CONCLUSION

Density functional theory's plane-wave pseudo-potential techniques have been used to investigate the electronic and optical characteristics of Cs-doped $FAPbI_3$. According to our DFT calculations, the bandgap of $FAPbI_3$ doped with 5% Cs was 0.98 eV, but the bandgap of 12.5% was 1.28 eV. The Shockley-Queisser optimum is reached by this band gap of 1.28 eV, suggesting that 12.5% Cs-doped $FAPbI_3$ ($Cs_{0.125}FA_{0.875}PbI_3$) may have a high PCE and be appropriate for tandem solar cells. A distinct bandgap and a high density of states at the band boundaries are shown in the DOS of $Cs_{0.125}FA_{0.875}PbI_3$. These characteristics help perovskite solar cells generate and transmit charge carriers efficiently. Higher photocurrent and increased solar cell power conversion efficiency may result from this. Both $FAPbI_3$ and 12.5% Cs-doped exhibit substantial visible-range absorption and a bandgap that is appropriate for photovoltaic applications, according to their absorption spectra. $Cs_{0.125}FA_{0.875}PbI_3$'s dielectric function and refractive index spectra show a bandgap of around 1.55 eV, dispersion with photon energy and polarization dependence, substantial absorption in particular energy ranges, and significant optical anisotropy. By regulating the orientation of the perovskite sheet and the polarization of light, these characteristics can be used to maximize the performance of perovskite solar cells. The anisotropy of the optical characteristics indicates that better light absorption and charge collection may be achieved by optimizing the device architecture. The graphs of optical properties show that 12.5% Cs doping has a major impact on $FAPbI_3$'s optical behaviour. The observed trends in dielectric function, JDOS, and absorption are in line with the enhanced optical characteristics and bandgap widening anticipated from Cs doping. As a result, $Cs_{0.125}FA_{0.875}PbI_3$ shows promise for customizing the material's bandgap for certain uses, including light-emitting diodes or tandem solar cells.

REFERENCES

Brakkee, R., & Williams, R. M. (2020). Minimizing defect states in lead halide perovskite solar cell materials. *Applied Sciences, 10*(9), 3061.

Cao, Y. *et al.* Unconventional superconductivity in magic-angle graphene superlattices. *Nature 556,* 43–50 (2018).

Duan, M., Wang, Y., Zhang, P., & Du, L. (2023). Effect of Cs+ Doping on the Carrier Dynamics of $MAPbI_3$ Perovskite. *Materials, 16*(17), 6064.

Duan, J., Ren, M., Gao, Y., Jia, X., Zhang, X., & Dong, Y. (2024). Enhancing performance of low-temperature fabricated inverted planar perovskite solar cells through triple-cation perovskite optimization. *Optical Materials, 156,* 115945.

Elmestekawy, K. A., Gallant, B. M., Wright, A. D., Holzhey, P., Noel, N. K., Johnston, M. B., ... & Herz, L. M. (2023). Photovoltaic performance of FAPbI3 perovskite is hampered by intrinsic quantum confinement. *ACS Energy Letters, 8*(6), 2543-2551.

Eperon, G. E., Stranks, S. D., Menelaou, C., Johnston, M. B., Herz, L. M., & Snaith, H. J. (2014). Formamidinium lead trihalide: a broadly tunable perovskite for efficient planar heterojunction solar cells. *Energy & Environmental Science, 7*(3), 982-988.

Giannozzi, P., Baseggio, O., Bonfà, P., Brunato, D., Car, R., Carnimeo, I., ... & Baroni, S. (2020). Quantum ESPRESSO toward the exascale. *The Journal of chemical physics, 152*(15).

Giannozzi, P., Andreussi, O., Brumme, T., Bunau, O., Nardelli, M. B., Calandra, M., ... & Baroni, S. (2017). Advanced capabilities for materials modelling with Quantum ESPRESSO. *Journal of physics: Condensed matter, 29*(46), 465901.

Giannozzi, P., Baroni, S., Bonini, N., Calandra, M., Car, R., Cavazzoni, C., ... & Wentzcovitch, R. M. (2009). QUANTUM ESPRESSO: a modular and open-source software project for quantum simulations of materials. *Journal of physics: Condensed matter, 21*(39), 395502.

Gregg, B. A. (2003). Excitonic solar cells. *The Journal of Physical Chemistry B, 107*(20), 4688-4698.

Imran, M., & Khan, N. A. (2019). Perovskite phase formation in formamidinium–methylammonium lead iodide bromide (FAPbI3) 1-x (MAPbBr3) x materials and their morphological, optical and photovoltaic properties. *Applied Physics A, 125*(8), 575.

Kaminski, P. M., Isherwood, P. J. M., Womack, G., & Walls, J. M. (2016). Optical optimization of perovskite solar cell structure for maximum current collection. *Energy Procedia, 102,* 11-18.

Li, D., Shi, J., Xu, Y., Luo, Y., Wu, H., & Meng, Q. (2018). Inorganic–organic halide perovskites for new photovoltaic technology. *National Science Review, 5*(4), 559-576.

Liang, Y., Li, F., Cui, X., Lv, T., Stampfl, C., Ringer, S. P., ... & Zheng, R. (2024). Toward stabilization of formamidinium lead iodide perovskites by defect control and composition engineering. *Nature Communications, 15*(1), 1707.

Liu, Y., Banon, J. P., Frohna, K., Chiang, Y. H., Tumen-Ulzii, G., Stranks, S. D., ... & Friend, R. H. (2022). The electronic disorder landscape of mixed halide perovskites. *ACS Energy Letters, 8*(1), 250-258.

Lu, H., Krishna, A., Zakeeruddin, S. M., Grätzel, M., & Hagfeldt, A. (2020). Compositional and interface engineering of organic-inorganic lead halide perovskite solar cells. *Iscience, 23*(8).

Martin, R. M. (2020). *Electronic structure: Basic theory and practical methods* (2nd ed.). Cambridge University Press.

Molas, M. R. (2023). Excitons and Phonons in Two-Dimensional Materials: From Fundamental to Applications. *Nanomaterials, 13*(23), 3047.

Momma, K., & Izumi, F. (2008). VESTA: a three-dimensional visualization system for electronic and structural analysis. *Journal of Applied crystallography, 41*(3), 653-658.

Monkhorst, H. J., & Pack, J. D. (1976). Special points for

Brillouin-zone integrations. *Physical review B, 13*(12), 5188.

Othman, M., Jeangros, Q., Jacobs, D. A., Futscher, M. H., Zeiske, S., Armin, A., ... & Hessler-Wyser, A. (2024). Alleviating nanostructural phase impurities enhances the optoelectronic properties, device performance and stability of cesium-formamidinium metal–halide perovskites. *Energy & Environmental Science, 17*(11), 3832-3847.

Perdew, J. P., Burke, K., & Ernzerhof, M. (1996). Generalized gradient approximation made simple. *Physical review letters, 77*(18), 3865.

Radzwan, A., Ahmed, R., Shaari, A., & Lawal, A. (2019). Ab initio calculations of optoelectronic properties of antimony sulfide nano-thin film for solar cell applications. *Results in Physics, 15,* 102762.

Regan, E. C. *et al.* Mott and generalized Wigner crystal states in WSe2/WS2 moiré superlattices. *Nature 579,* 359–363 (2020).

Saleh, M. H., Jafar, M. M. A. G., Bulos, B. N., & Al-Daraghmeh, T. M. (2014). Determination of optical properties of undoped amorphous selenium (a-Se) films by dielectric modeling of their normal-incidence transmittance spectra. *Applied Physics Research, 6*(6), 10.

Shen, X. P., Lin, J. B., Hu, R. Y., Liu, Y. C., Xu, L. Q., Niu, H. B., ... & Wang, V. (2024). Compositional effects on structural, electronic, elastic, piezoelectric and dielectric properties of GaInN alloys: a first-principles study. *RSC advances, 14*(10), 6752-6761.

Srathongsian, L., Kaewprajak, A., Naikaew, A., Seriwattanachai, C., Phuphathanaphong, N., Inna, A., ... & Kanjanaboos, P. (2024). Cs and Br tuning to achieve ultralow-hysteresis and high-performance indoor triple cation perovskite solar cell with low-cost carbon-based electrode. *Iscience, 27*(4).

Subedi, B., Li, C., Chen, C., Liu, D., Junda, M. M., Song, Z., ... & Podraza, N. J. (2022). Urbach energy and open-circuit voltage deficit for mixed anion–cation perovskite solar cells. *ACS Applied Materials & Interfaces, 14*(6), 7796-7804.

Taya, A., Rani, P., Thakur, J., & Kashyap, M. K. (2019). First principles study of structural, electronic and optical properties of Cs-doped $CH_3NH_3PbI_3$ for photovoltaic applications. *Vacuum, 160,* 440-444.

Virtual Lab Inc. (2017, January 1). *Materials Square.* https://www.materialssquare.com/

Weller, M. T., Weber, O. J., Frost, J. M., & Walsh, A. (2015). Cubic perovskite structure of black formamidinium lead iodide, α-$[HC(NH_2)_2]PbI_3$, at 298 K. *The Journal of Physical Chemistry Letters, 6*(16), 3209–3212.

Wright, A. D., Volonakis, G., Borchert, J., Davies, C. L., Giustino, F., Johnston, M. B., & Herz, L. M. (2020). Intrinsic quantum confinement in formamidinium lead triiodide perovskite. *Nature Materials, 19*(11), 1201-1206.

Wu, Y., Chen, W., Chen, G., Liu, L., He, Z., & Liu, R. (2018). The impact of hybrid compositional film/structure on organic–inorganic perovskite solar cells. *Nanomaterials, 8*(6), 356.

Xu, Y. *et al.* Correlated insulating states at fractional fillings of moiré superlattices. *Nature 587,* 214–218 (2020).

Zhang, T., Xu, Q., Xu, F., Fu, Y., Wang, Y., Yan, Y., ... & Zhao, Y. (2019). Spontaneous low-temperature crystallization of α-FAPbI3 for highly efficient perovskite solar cells. *Science Bulletin, 64*(21), 1608-1616.

Zhang, Y., Yang, T., Lee, S. U., Liu, S., Zhao, K., & Park, N. G. (2023). Stabilizing α-Phase FAPbI3 Perovskite Induced by an Ordered Solvated Quasi-Crystalline PbI2. *ACS Energy Letters, 9*(1), 159-167.

Zheng, Z., Wang, S., Hu, Y., Rong, Y., Mei, A., & Han, H. (2022). Development of formamidinium lead iodide-based perovskite solar cells: efficiency and stability. *Chemical Science, 13*(8), 2167-2183.